3. K. Towe, *Science* **157**, 1048 (1967).
4. D. M. Raup, *J. Geol.* **67**, 661 (1959).
5. S. Weiner, L. Addadi, H. Wagner, *Mater. Sci. Eng.* **11**, 1 (2000).
6. S. Loven, *Sven. Vetensk. Akad. Handl.* **18**, 1 (1892).
7. W. B. Carpenter, *Brit. Assoc. Adv. Sci. London Rep.* **17**, 93 (1847).
8. K. Okazaki, *Embryologia (Nagoya)* **5**, 283 (1960).
9. J. B. Pilkington, *J. Mar. Biol. Assoc. UK* **49**, 857 (1969).
10. K. Märkel, U. Röser, *Zoomorphology* **103**, 25 (1983).
11. K. Märkel, U. Röser, M. Stauber, *Zoomorphology* **109**, 79 (1989).
12. F. H. Wilt, *Zool. Sci.* **19**, 253 (2002).
13. E. Beniash, J. Aizenberg, L. Addadi, S. Weiner, *Proc. R. Soc. London B Biol. Sci.* **264**, 461 (1997).
14. E. Beniash, L. Addadi, S. Weiner, *J. Struct. Biol.* **125**, 50 (1999).
15. I. M. Weiss, N. Tuross, L. Addadi, S. Weiner, *J. Exp. Zool.* **293**, 478 (2002).
16. K. Märkel, U. Röser, *Zoomorphology* **103**, 43 (1983).
17. B. M. Heatfield, *J. Exp. Zool.* **178**, 233 (1971).
18. P. Dubois, C. P. Chen, *Echinoderm Stud.* **3**, 109 (1989).
19. P. Dubois, L. Ameye, *Microsc. Res. Tech.* **55**, 427 (2001).
20. L. Brecevic, N. A. *J. Cryst. Growth* **98**, 504 (1989).
21. F. Lippmann, *Sedimentary Carbonate Minerals* (Springer, Berlin, 1973).
22. Materials and methods are available as supporting material on *Science* Online.
23. L. Addadi, S. Raz, S. Weiner, *Adv. Mat.* **15**, 959 (2003).
24. S. Raz, P. C. Hamilton, F. H. Wilt, S. Weiner, L. Addadi, *Adv. Funct. Mater.* **13**, 480 (2003).
25. A. Berman, L. Addadi, S. Weiner, *Nature* **331**, 546 (1988).
26. G. F. Xu, N. Yao, I. A. Aksay, J. T. Groves, *J. Am. Chem. Soc.* **120**, 11977 (1998).
27. J. Aizenberg, J. L. Grazul, D. A. Muller, D. R. Hamann, *Science* **299**, 1205 (2003).
28. L. B. Gower, D. J. Odom, *J. Cryst. Growth* **4**, 719 (2000).
29. E. Loste, F. C. Meldrum, *Chem. Commun.*, 901 (2001).
30. We thank M. Cohen for help with the ESEM measurements. We also thank B. Scharfstein, I. Ivry, and Y. Raz (SeaOr Marine Enterprises Ltd.) for providing the animals and facilities for spine regeneration. L.A. is the incumbent of the Dorothy and Patrick Gorman Professorial Chair of Biological Ultrastructure, and S.W. is the incumbent of the Dr. Trude Burchardt Professorial Chair of Structural Biology. Supported by a grant from the Philip Klutznick Research Fund.

Supporting Online Material

www.sciencemag.org/cgi/content/full/306/5699/1161/DC1
Materials and Methods

2 July 2004; accepted 6 October 2004

Earth Tides Can Trigger Shallow Thrust Fault Earthquakes

Elizabeth S. Cochran,[1]* John E. Vidale,[1] Sachiko Tanaka[2]†

We show a correlation between the occurrence of shallow thrust earthquakes and the occurrence of the strongest tides. The rate of earthquakes varies from the background rate by a factor of 3 with the tidal stress. The highest correlation is found when we assume a coefficient of friction of $\mu = 0.4$ for the crust, although we see good correlation for μ between 0.2 and 0.6. Our results quantify the effect of applied stress on earthquake triggering, a key factor in understanding earthquake nucleation and cascades whereby one earthquake triggers others.

For more than a century, researchers have sought to detect the effect on the timing of earthquakes of the gravitational perturbations on Earth from the Moon and Sun (*1*). However, the tidal stresses in most locations are small, and usually it is difficult to ascertain the orientation of the fault plane, which is critical when calculating the effect of the stress variations. Earthquake-tide correlations have been observed to be small or nonexistent in normal crust (*2–4*); however, correlations have been shown in shallow, possibly hydrothermal or magma-related areas (*5*, *6*). Here, we take advantage of accurate accounting of ocean tides (*7*) and a large data set of earthquake focal mechanisms with fairly well known fault planes (*8*) to look for a correlation.

We used global earthquakes in the Harvard Centroid Moment Tensor (CMT) catalog (*9*). For each event, we calculated a tidal-stress time series that includes the solid Earth tide and an ocean-loading component (*7*, *10*, *11*). Solid-Earth tides induce stresses only up to 5×10^3 Pa (0.05 bar), whereas in ocean basins, water loading builds stresses up to nearly 5×10^4 Pa (0.5 bar). Both components must be accurately determined to fully resolve tidal influences on the initiation of earthquakes globally. We resolved tidal stresses into normal and shear stress acting on each of the two possible fault planes of the CMT earthquake focal mechanism. Shear failure under compressive stress can be described by the Coulomb criterion, in which a fault fails under a combination of shear and normal stress: $\tau_c = \tau + \mu\sigma_n$, where τ and σ_n are the shear and normal stresses, respectively, and μ is the coefficient of friction. In addition to examining shear and normal stress independently, we tested different values of μ (0.2, 0.4, or 0.6). For each event, we calculated the tidal phase angle (θ) between –180° and 180° (*11*); 0° phase is defined to be at the time of maximum stress that can promote failure, which is extensional for normal stress and in the direction of slip for shear stress (Fig. 1). In addition, we defined the average of the tidal stress amplitudes at the peaks just before and after each earthquake (τ_{pb} and τ_{pa}, respectively) to be the peak tidal stress τ_p.

We focused on a subset of shallow thrust earthquakes with depths of 0 to 40 km because these earthquakes are in regions with the

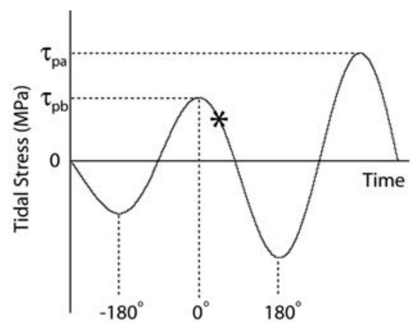

Fig. 1. Schematic diagram of the tidal stress time series spanning 1 day for a hypothetical earthquake (asterisk). Tidal phase is marked, with the maximum Coulomb stress promoting failure defined at 0° phase. The earthquake occurs at $\theta = 45°$. Peak stress amplitudes before and after an event (τ_{pb} and τ_{pa}, respectively) are averaged to determine τ_p.

Table 1. Comparison of coefficients of friction. Data are shown for the 250 events with the highest calculated tidal stress (τ_p) given different values of the coefficient of friction (μ). Binomial is approximated by a Gaussian distribution; *P* values are determined using Schuster's statistical test of data distribution (values below 5% are often considered significantly nonrandom). θ_{peak} is the phase of the peak of a sinusoidal fit to the data. See text for definition of N_{ex}.

Events	Binomial (%)	*P* value (%)	N_{ex} (%)	θ_{peak} (degrees)
$\mu = 0$ (shear)	4.38	10.36	5.6	–22.2
$\mu = 0.2$	0.1439	0.6253	9.6	–1.2
$\mu = 0.4$	0.0032	0.0157	12.8	0.2
$\mu = 0.6$	0.0942	0.3265	10.0	6.0
$\mu = \infty$ (normal)	0.4688	3.677	8.4	15.8

[1]Department of Earth and Space Sciences and Institute of Geophysics and Planetary Physics, University of California, Los Angeles, CA 90095, USA. [2]Department of Geophysics, Graduate School of Science, Tohoku University, Sendai, Miyagi 980-8578, Japan.

*To whom correspondence should be addressed. E-mail: cochran@moho.ess.ucla.edu
†Present address: National Research Institute for Earth Science and Disaster Prevention (NIED), Tsukuba-shi, Ibaraki-ken 305, Japan.